



Published in final edited form as:

Nature. ; 476(7359): 170–175. doi:10.1038/nature10336.

The landscape of recombination in African Americans

A full list of authors and affiliations appears at the end of the article.

Abstract

Recombination, together with mutation, is the ultimate source of genetic variation in populations. We leverage the recent mixture of people of African and European ancestry in the Americas to build a genetic map measuring the probability of crossing-over at each position in the genome, based on about 2.1 million crossovers in 30,000 unrelated African Americans. At intervals of more than three megabases it is nearly identical to a map built in Europeans. At finer scales it differs significantly, and we identify about 2,500 recombination hotspots that are active in people of West African ancestry but nearly inactive in Europeans. The probability of a crossover at these hotspots is almost fully controlled by the alleles an individual carries at *PRDM9* ($P < 10^{-245}$). We identify a 17 base pair DNA sequence motif that is enriched in these hotspots, and is an excellent match to the predicted binding target of African-enriched alleles of *PRDM9*.

In humans and many other species, recombination is not evenly distributed across the genome, but instead occurs in “hotspots”: two kilobase (kb) segments where the crossover rate is far higher than in the flanking DNA sequence^{1,2,3}. The highest resolution genetic map in contemporary humans to date, the “deCODE Map”, is based on about 500,000 crossovers identified in 15,000 Icelandic meioses⁴. However, a limitation of maps built in people of European descent^{4,5,6} is that they may not apply equally well in other populations, as suggested by comparisons of maps across ethnic groups^{4,7,8,9} and patterns of linkage disequilibrium (LD) breakdown which suggest that more of the genome may be recombinationally active in West Africans¹⁰. It is known that a major determinant of the positions of recombination hotspots is *PRDM9*, a meiosis-specific histone H3 methyltransferase whose zinc finger (ZF) domain binds DNA sequence motifs^{11,12,13}. In Europeans, *PRDM9* ZF arrays are predominantly of two similar types, “A” and “B”, both of which bind the 13-bp motif CCNCCNTNCCNC¹¹. In contrast, 36% of West African

Users may view, print, copy, download and text and data- mine the content in such documents, for the purposes of academic research, subject always to the full Conditions of use: http://www.nature.com/authors/editorial_policies/license.html#terms

Correspondence should be addressed to: Anjali G. Hinch (anjali@well.ox.ac.uk); David Reich (reich@genetics.med.harvard.edu) or Simon R. Myers (myers@stats.ox.ac.uk).

*These authors equally directed the research

AUTHOR CONTRIBUTIONS

DR and SRM conceived the study. AGH, AT, NP, YS, NR, CDP, GKC, KW, SGB, DR and SRM performed analyses. NR performed the experimental work (genotyping of polymorphisms at *PRDM9*). AGH, NP, JNH, BEH, HAT, ALP, HH, SJC, CAH, JGW, DR and SRM coordinated the study. AGH, DR and SRM wrote the paper. NR, CDP, GKC, KW, SGB, SR, JNH, BEH, HAT, HH, CJC, CAH, JGW, DR and all the alphabetically listed authors contributed to sample collection and generation of SNP array data. All authors contributed to revision and review of the manuscript.

AUTHOR INFORMATION

Crossover rate estimates for the AA Map, Pedigree Map, AE Map and S Map can be found at <http://www.well.ox.ac.uk/~anjali/AAmap/>. We also provide estimates of uncertainty for each map based on samples from the Markov Chain Monte Carlo. Association testing results for each SNP are available from the authors on request.

alleles are not of the A or B type^{9,13}. Sperm typing of males who carry neither the A nor the B allele has shown no evidence of crossover activity at recombination hotspots associated with the 13-bp motif⁹.

To investigate differences in the crossover landscape across human populations, we built a genetic map in African Americans, who have an average of about 80% West African and 20% European ancestry, leading to genomes comprised of multi-megabase stretches of either West African or European ancestry¹⁴. Computational approaches, including HAPMIX¹⁵, have been developed to infer the probability of 0, 1 or 2 European or African alleles at each locus in individuals genotyped at hundreds of thousands of single nucleotide polymorphisms (SNPs)^{15,16,17}. Positions where the inferred number of European or African alleles changes reflect crossover events that have occurred since admixture began (on average six generations ago¹⁵). The change in the probability of European ancestry between adjacent SNPs can be interpreted as the probability of such a crossover between them. We inferred crossover events in 29,589 apparently unrelated African Americans who had been genotyped on SNP arrays in genetic association studies (Methods; Figure 1A). To minimize false-positive crossovers, we restricted to crossovers that HAPMIX inferred with probability of >95%, and that were flanked by a minimum of 2 centimorgan (cM) stretches where the ancestry was inferred to be unchanging (Note S1). This produced 2,113,293 highconfidence crossovers, with a typical switch point resolved within 70kb with probability 50% (Note S1).

To build a high resolution African American genetic map (AA Map), we leveraged the fact that most crossovers occur in hotspots shared across individuals¹ (Methods). Intuitively, while any crossover can only be roughly localized, inter-SNP intervals that are inferred to have an appreciable probability of crossover in multiple individuals are likely to contain recombination hotspots, allowing much better localization (Figure S1). To implement this idea, we modeled the recombination rate for each inter-SNP interval as shared across individuals, and used a Markov Chain Monte Carlo (MCMC) to sample rates consistent with the data (Methods). This provides well-calibrated estimates of the crossing-over rate between all pairs of markers as well as estimates of rate uncertainty (Note S1 and Figure S2). We find that the interval size at which the average recombination rate is equal to the standard error is 6 kb, which is the same accuracy that would be expected from a map based on 500,000 crossovers whose boundaries were precisely resolved (Note S1). Despite this high resolution, there are also some limitations. First, the AA Map does not separately infer male and female recombination rates (it is a sex-averaged map) and requires normalization by the total map length (like LD maps^{3,18}). Second, the map has less resolution and may miss a higher fraction of true crossovers at loci where it is more difficult to detect and resolve crossovers due to low SNP density or low differentiation between West Africans and Europeans. Third, the map may be biased where ancestry deviates from the average, for example at 8q24, where the 10% of the people in this study who have prostate cancer have an elevated proportion of African ancestry¹⁹. Fourth, the map assumes that all individuals are unrelated, whereas in fact there is likely some shared ancestry, resulting in multiple counting of some crossovers and an overestimate of map precision.

To assess the accuracy of the AA Map, we generated an independent African American pedigree map by analyzing 222 nuclear families that included 1,056 meioses in which we

could directly detect crossovers between parent and child (Methods; Figure 1A). Examination of the AA Map rate around directly detected crossovers confirms the high resolution: the rate around such crossovers shows at least as strong a peak as that observed in maps based on LD^{2,3,18} (Figure S3). We next computed correlation coefficients for both the AA Map and the deCODE Map⁴ to maps derived from the breakdown of LD in Europeans (CEU) and West Africans (YRI)¹⁸. At broad scales (>3 Mb) they are almost identical ($\rho > 0.97$; Table 1) At fine scales, the AA Map is more accurate (Table 1 and Table S1), as reflected in a modest improvement in correlation to the CEU Map at a 3kb scale ($\rho_{AA,CEU(3kb)} = 0.66$ vs. $\rho_{deCODE,CEU(3kb)} = 0.58$), and a major improvement for the YRI Map ($\rho_{AA,YRI(3kb)} = 0.71$ vs. $\rho_{deCODE,YRI(3kb)} = 0.53$). The deCODE Map is more correlated to the CEU Map than to the YRI Map at scales <1 Mb, suggesting that this map, built in Icelanders, reflects more European recombination rates. The AA Map shows the opposite pattern, suggesting that it reflects more West African recombination patterns.

We compared the rate estimates for all four maps (AA, deCODE, CEU and YRI) over a 200 kb region within the MHC locus where recombination rates in European males have been characterized through sperm typing¹ (Figure 1B). The AA Map detects five of six known hotspots, and localizes them to within 1 kb (the sixth hotspot is weak, with a peak male rate below the genome average¹). Strikingly, the two maps based on samples with African ancestry (AA and YRI) found a hotspot not present in either map based on samples of European ancestry (deCODE and CEU) (Figure 1C; Figure S4 gives a second example). We confirmed that such “African-enriched” hotspots also occur genome-wide, by examining 2,375 loci with recombination rate peaks in the YRI Map (>5 cM/Mb) but not the CEU Map (<1 cM/Mb), and finding a rate rise in the independently generated AA Map, but not in the deCODE Map (Figure S5A). In the reciprocal experiment searching for European-specific hotspots, we find no such evidence for genuine ancestry specificity; at loci with recombination rate peaks in the CEU Map but not the YRI Map, there are weak peaks in both the deCODE and AA maps (Methods; Figure S5B). Thus, hotspots active in Europeans are consistently “shared” with YRI and African Americans, while populations with African ancestry harbor additional, non-shared hotspots we call “African-enriched”.

To understand the features of recombination in West Africans that differ from Europeans, we estimated the degree to which each African American person’s crossovers occur in “African-enriched” hotspots, compared with “Shared” hotspots, a phenotype we refer to as their “African-enrichment” (AE). We view each individual’s crossovers as sampled from a mixture of two genetic maps—an “S Map” of shared hotspots based on the deCODE Map, and an “AE Map” of African-enriched hotspots that is learned from comparing the deCODE and AA Maps—so that the proportion of crossovers assigned to the AE Map is a person’s AE phenotype (Note S4). We tested approximately 3 million SNPs (genotyped and imputed) for association with three phenotypes: AE, usage of LD-based hotspots known to be enriched for the 13-bp motif CCNCCNTNCCNC²⁰, and genome-wide crossover rate (in pedigrees) (Methods and Note S4). In crossovers detected in unrelated African Americans, the alleles a person carries are only sometimes descended from the ancestor in whom the crossover occurred, thus adding noise to the association signal (nevertheless there is useful signal given the large sample size; Note S4). In the Pedigree Map, association between alleles and AE can be tested directly because we have genotypes in the parents.

The SNP showing the strongest association with AE is rs6889665 ($P=1.5\times 10^{-246}$; Figure 2A, Figure S6), which has a derived allele frequency of 29% in YRI and 2% in CEU, and is within 4 kb of the ZF array of *PRDM9*^{4,9,11,12,13}. This SNP is associated with AE in both the pedigree individuals and the unrelated individuals (Note S4), and is also the SNP most strongly associated with usage of LD-based hotspots ($P=1.8\times 10^{-52}$) (Table S2). No locus outside *PRDM9* is significant ($P<0.01$ after Bonferroni correction; Table S3). To better understand the association at rs6889665, we inferred the alleles in the *PRDM9* ZF array carried by 139 individuals based on sequencing data from the 1000 Genomes Project²¹, using the reads to infer each individual's *PRDM9* alleles among 29 alleles whose full sequences were previously determined⁹ (Note S5). Grouping *PRDM9* alleles based on how closely their binding target predictions match the 13-bp motif, following Berg et al.⁹, we find that the ancestral "T" variant at rs6889665 is strongly correlated to "8/8 matches" to the 13-bp motif (including the "A" and "B" alleles), while the derived "C" variant is almost perfectly correlated to a group of "5/8 match" alleles, all predicted to bind a common, different, 17-bp motif "CCgCNgtNNNCgtNNCC"⁹. This implies a common historical origin for alleles matching this 17-bp motif (Figure 2B; Figure S7; Note S5). We also experimentally measured the number of zinc fingers in *PRDM9* in 354 individuals including 166 African Americans from the pedigree study (Methods). This showed, again, that rs6889665 differentiates *PRDM9* alleles into two different classes, with 96% of haplotypes carrying the ancestral allele having <14 zinc fingers, and 93% of haplotypes carrying the derived allele having 14 zinc fingers (Figure S7). After conditioning on rs6889665, there is no evidence that ZF length is associated with the AE phenotype. Several SNPs near the *PRDM9* ZF array show a conditional association signal that is much weaker than rs6889665, but still significant (Figure 2C; Figure S6; Note S4), with the strongest at rs10043097 ($P=8.3\times 10^{-14}$), upstream of the *PRDM9* transcription start site. These SNPs may tag additional variation in *PRDM9* ZF array, or potentially expression levels.

To directly identify candidate African-enriched hotspot motifs, we selected 2,454 loci with a high crossover rate in the AE Map and YRI Map ($>2\text{cM}/\text{Mb}$ over 2kb), and no more than half this rate in the S Map and CEU Map (this set is more powerfully enriched for higher recombination in people of African ancestry than the 2,375 above, as it includes information from the contemporary maps). We compared these to a "control set" of 7,328 candidate hotspots more active in the European than the African derived maps (Methods; Note S6). To identify sequence motifs associated with the African-enriched hotspots^{3,22}, we identified short motifs that occurred at increased frequency in the African-enriched hotspot set (Note S6). Testing all motifs of length 5–9 bases revealed a 9-mer "CCCCAGTGA" (OR=1.79, $P=2.24\times 10^{-8}$, Bonferroni corrected $P=0.004$) which exhibited a kilobase-scale rate peak near occurrences of this motif in African derived maps, but in neither of the European derived maps (Figure S8). Further analysis revealed a strong influence of downstream flanking bases (Figure S9), and degeneracy, yielding a 17-bp consensus sequence "CCCCaGTGAGCGTtgCc" (Figure 3A; more strongly signaled bases are uppercase) with the same consensus obtained when we considered flanking sequence for only odd or even chromosomes, and whether we based the analysis on AE-S or YRI-CEU map comparisons (Note S6). The 500 best matches to this motif have a ~3-fold increase in average rate in the AA and YRI relative to the deCODE and CEU maps (Figure 3B, Figure S8). Hotspots

associated with the motif occur in both unique and repetitive DNA (e.g. L1PA10/13 LINE elements; Figure S10) (Note S6). We also compared the 17-bp consensus to the binding motif predicted for “5/8 match” alleles, and found that they match almost precisely (Figure 3A; 10 of 11 bases, $P=8.1\times 10^{-6}$).

How much of the African-enriched recombination pattern can be explained by *PRDM9*? We estimated the fraction of variation in the AE phenotype explained by rs6889665 in our pedigree data after accounting for noise in the phenotype estimation (Note S4). Over 82% of map usage variability is explained by rs6889665 genotype alone. Given there are further influential *PRDM9* variants (Figure 3C), this gene may thus explain almost all differences in local rate between the West African and European populations. We next examined rates around 82 narrowly defined (<10kb) crossover sites in 7 individuals homozygous for the derived allele at rs6889665. There is no evidence of hotspots at these loci in either the deCODE or CEU Maps (Figure 3C), in contrast to events in individuals carrying the ancestral allele at rs6889665 (Figure S11). Thus, crossover positions in individuals who are homozygous for the derived allele at rs6889665 are consistent with an entirely different recombination hotspot landscape, which would imply *PRDM9* control of all hotspots⁹. Despite the strong correlation between maps at megabase scales, there is mounting evidence that *PRDM9*'s influence on crossing-over may not be limited to fine scales^{4,11}: we observe a weakly significant association of rs6889665 with the total number of crossovers genome-wide in pedigrees ($P=0.04$), corresponding to an average 1.3 crossovers more per meiosis per derived allele, exceeding the strongest previously known association²³ at *RNF212*.

We have shown that *PRDM9* alleles that bind a novel 17-bp motif and occur at greatly increased frequency in people of West African ancestry have led to a shift in the recombination landscape compared with people of non-African ancestry. The larger number of hotspots available to West Africans implies that at the population level, crossovers are more evenly distributed than in Europeans¹⁰, and thus the shorter extent of West African LD is not due to differences in demographic history alone (such as the lack of an out-of-Africa founder event)²⁴. Our findings also have medical implications, as recombination errors leading to insertions or deletions are known to be associated with recombination hotspots^{9,22,25}. Our results predict that the congenital abnormalities that have been associated with the recombination hotspots bound by *PRDM9* “A” and “B” alleles will occur at a decreased rate in people of West African ancestry, whereas new diseases will arise due to recombination errors near African-enriched hotspots.

METHODS SUMMARY

We assembled SNP array data from 29,589 unrelated people and 222 nuclear families genotyped at 490,000–910,000 SNPs from the Candidate Gene Association Resource (CARE), studies at the Children’s Hospital of Philadelphia (CHOP), the African American Breast Cancer Consortium, the African American Prostate Cancer Consortium and the African American Lung Cancer Consortium. To build a recombination map, we used HAPMIX to localize candidate crossover positions¹⁵, and implemented a Markov Chain Monte Carlo (MCMC) that used the probability distributions for the positions of the filtered crossovers to infer recombination rates for each of 1.3 million inter-SNP intervals. We also

implemented a second MCMC that models each individual's set of crossovers as a mixture of a Shared (S) Map similar to the European deCODE Map and an African-enriched (AE) Map, and then assigns each individual an "AE phenotype" corresponding to the proportion of their newly detected crossovers assigned to the AE Map. We imputed genotypes at up to three million HapMap2 SNPs⁸ using MaCH²⁶, and then tested each of these SNPs for association with the AE phenotype and other recombination-related phenotypes. We identified 2,454 candidate African-enriched hotspots with increased recombination rates in the YRI vs. CEU maps, and in the AE vs. S maps, and searched for motifs enriched at these loci, thus identifying a degenerate 17-bp motif. To study the structure of *PRDM9*, we measured the length of the *PRDM9* zinc finger array and genotyped rs6889665 in YRI, CEU and the CARE nuclear families; we also carried out imputation based on 1000 Genomes Project short read data¹⁰ to infer the alleles individuals carry, among 29 previously characterized in a sequencing study of *PRDM9*⁹.

Supplementary Material

Refer to Web version on PubMed Central for supplementary material.

Authors

Anjali G. Hinch¹, Arti Tandon^{2,3}, Nick Patterson², Yunli Song⁴, Nadin Rohland^{2,3}, Cameron D. Palmer^{5,6}, Gary K. Chen⁷, Kai Wang^{8,9}, Sarah G. Buxbaum¹⁰, Meggie Akyzbekova^{10,11}, Melinda C. Aldrich^{12,13}, Christine B. Ambrosone¹⁴, Christopher Amos¹⁵, Elisa V. Bandera¹⁶, Sonja I. Berndt¹⁷, Leslie Bernstein¹⁸, William J. Blot^{13,19}, Cathryn H. Bock²⁰, Eric Boerwinkle²¹, Qiuyin Cai¹³, Neil Caporaso¹⁷, Graham Casey⁷, L. Adrienne Cupples²², Sandra L. Deming¹³, W. Ryan Diver²³, Jasmin Divers²⁴, Myriam Fornage²⁵, Elizabeth M. Gillanders²⁶, Joseph Glessner⁹, Curtis C. Harris²⁷, Jennifer J. Hu²⁸, Sue A. Ingles⁷, Williams Isaacs²⁹, Esther M. John³⁰, W. H. Linda Kao³¹, Brendan Keating⁹, Rick A. Kittles³², Laurence N. Kolonel³³, Emma Larkin³⁴, Loic Le Marchand³³, Lorna H. McNeill³⁵, Robert C. Millikan³⁶, Adam Murphy³⁷, Solomon Musani¹¹, Christine Neslund-Dudas³⁸, Sarah Nyante³⁶, George J. Papanicolaou³⁹, Michael F. Press⁷, Bruce M. Psaty⁴⁰, Alex P. Reiner⁴¹, Stephen S. Rich⁴², Jorge L. Rodriguez-Gil²⁸, Jerome I. Rotter⁴³, Benjamin A. Rybicki³⁸, Ann G. Schwartz²⁰, Lisa B. Signorello^{13,19}, Margaret Spitz¹⁵, Sara S. Strom⁴⁴, Michael J. Thun²³, Margaret A. Tucker¹⁷, Zhaoming Wang⁴⁵, John K. Wiencke⁴⁶, John S. Witte⁴⁷, Margaret Wrensch⁴⁶, Xifeng Wu¹⁵, Yuko Yamamura⁴⁴, Krista A. Zanetti^{26,27}, Wei Zheng¹³, Regina G. Ziegler¹⁷, Xiaofeng Zhu⁴⁸, Susan Redline⁴⁹, Joel N. Hirschhorn^{5,6,50}, Brian E. Henderson⁷, Herman A. Taylor Jr.^{11,51,52}, Alkes L. Price⁵³, Hakon Hakonarson^{9,54}, Stephen J. Chanock¹⁷, Christopher A. Haiman⁷, James G. Wilson⁵⁵, David Reich^{2,3,*}, and Simon R. Myers^{1,4,*}

Affiliations

¹Wellcome Trust Centre for Human Genetics, Oxford University, Roosevelt Drive, Oxford OX3 7BN, UK

²Broad Institute of MIT and Harvard, 7 Cambridge Center, Cambridge, MA 02142, USA

³Dept. of Genetics, Harvard Medical School, New Research Bldg., 77 Ave. Louis Pasteur, Boston, MA 02115, USA

⁴Department of Statistics, Oxford University, 1 South Parks Road, Oxford OX1 3TG, UK

⁵Program in Medical and Population Genetics, Broad Institute, 7 Cambridge Center, Cambridge, MA 02142, USA

⁶Div. of Genetics & Endocrinology and Program in Genomics, Childrens Hospital Boston, MA 02115, USA

⁷Department of Preventive Medicine and Department of Pathology, Keck School of Medicine, University of Southern California/ Norris Comprehensive Cancer Center, Los Angeles, CA 90033, USA

⁸Zilkha Neurogenetic Institute, University of Southern California, Los Angeles, CA 90089

⁹Center for Applied Genomics, The Childrens Hospital of Philadelphia, Philadelphia, Pennsylvania 19104, USA.

¹⁰Jackson Heart Study Coordinating Center, Jackson State University, 350 W. Woodrow Wilson Ave., Suite 701, Jackson, MS 39213, USA

¹¹Department of Medicine, University of Mississippi Medical Center, 2500 N. State St., Jackson, MS 39216, USA

¹²Department of Thoracic Surgery, Vanderbilt University School of Medicine, Nashville, TN 37203, USA

¹³Division of Epidemiology in the Department of Medicine, Vanderbilt Epidemiology Center; and the Vanderbilt-Ingram Cancer Center, Vanderbilt University School of Medicine, Nashville, TN 37203, USA

¹⁴Department of Cancer Prevention and Control, Roswell Park Cancer Institute, Buffalo, NY 14263, USA

¹⁵Department of Epidemiology, Division of Cancer Prevention and Population Sciences, The University of Texas MD Anderson Cancer Center, Houston, TX 7703

¹⁶The Cancer Institute of New Jersey, New Brunswick, NJ 08903, USA

¹⁷Division of Cancer Epidemiology and Genetics, National Cancer Institute, Bethesda, MD 20892, USA

¹⁸Division of Cancer Etiology, Dept. of Population Science, Beckman Research Inst., City of Hope, CA 91010, USA

¹⁹International Epidemiology Institute, Rockville, MD 20850, USA

- ²⁰Karmanos Cancer Institute and Dept. of Oncology, Wayne State University of Medicine, Detroit, MI USA 48201
- ²¹Human Genetics Center and Division of Epidemiology, University of Texas at Houston, 1200 Herman Pressler St., Houston, Texas 77030, USA
- ²²Department of Biostatistics, Boston University School of Public Health, 801 Massachusetts Avenue, Boston, MA 02118 and Framingham Heart Study, Framingham, MA 01702, USA
- ²³Epidemiology Research Program, American Cancer Society, Atlanta, GA 30303, USA
- ²⁴Department of Biostatistical Sciences, Wake Forest University School of Medicine WC-2326, Medical Center Blvd., Winston Salem, NC 27157, USA
- ²⁵Institute of Molecular Medicine and Division of Epidemiology, School of Public Health, University of Texas Health Sciences Center at Houston, 1825 Pressler Street, Houston, TX 77030, USA
- ²⁶Division of Cancer Control and Population Sciences, National Cancer Institute, Bethesda, MD 20892, USA
- ²⁷Laboratory of Human Carcinogenesis, Center for Cancer Research, National Cancer Institute, Bethesda, MD 20892, USA
- ²⁸Sylvester Comprehensive Cancer Center and Department of Epidemiology and Public Health, University of Miami Miller School of Medicine, Miami, FL 33136, USA
- ²⁹James Buchanan Brady Urological Institute, Johns Hopkins Hospital and Medical Institutions, Baltimore, MD 21287, USA
- ³⁰Cancer Prevention Institute of California, Fremont, CA 94538; and Stanford University School of Medicine and Stanford Cancer Center, Stanford, CA 94305, USA
- ³¹Department of Epidemiology, Johns Hopkins Bloomberg School of Public Health, 615 N. Wolfe St., Baltimore, MD 21205, USA
- ³²Department of Medicine, University of Illinois at Chicago, Chicago, IL 60607, USA
- ³³Epidemiology Program, University of Hawaii Cancer Center, Honolulu, HI 96813, USA
- ³⁴Department of Medicine, Division of Allergy, Pulmonary and Critical Care, 6100 Medical Center East, Vanderbilt University Medical Center, Nashville, TN 37232-8300, USA
- ³⁵Department of Health Disparities Research, Division of OVP, Cancer Prevention and Population Sciences, and Center for Community Implementation and Dissemination Research, Duncan Family Institute, The University of Texas MD Anderson Cancer Center, Houston, TX 77030, USA

- ³⁶Department of Epidemiology, Gillings School of Global Public Health, and Lineberger Comprehensive Cancer Center, University of North Carolina, Chapel Hill, NC 27599, USA
- ³⁷Department of Urology, Northwestern University, Chicago, IL 60611, USA
- ³⁸Department of Public Health Sciences, Henry Ford Hospital, Detroit, MI USA
- ³⁹Division of Cardiovascular Sciences, National Heart, Lung and Blood Institute, 6701 Rockledge Drive, Bethesda, MD 20892, USA
- ⁴⁰Cardiovascular Health Research Unit, Depts. of Medicine, Epidemiology & Health Services, Univ. of Washington; Group Health Research Institute; Group Health Cooperative; 1730 Minor Ave., Seattle, WA 98101, USA
- ⁴¹Department of Epidemiology, University of Washington, Box 357236 Seattle, WA 98195, USA
- ⁴²Center for Public Health Genomics, University of Virginia, West Complex Room 6111, Charlottesville, VA 22908, USA
- ⁴³Medical Genetics Institute, Cedars-Sinai Medical Center, 8700 Beverly Blvd, Los Angeles, CA 90048, USA
- ⁴⁴Department of Epidemiology, The University of Texas M. D. Anderson Cancer Center, Houston, TX 77030, USA
- ⁴⁵Core Genotype Facility, SAIC-Frederick, Inc., National Cancer Institute-Frederick, Frederick, Maryland, USA 20877, USA
- ⁴⁶University of California San Francisco, San Francisco CA 94158, USA
- ⁴⁷Institute for Human Genetics, Departments of Epidemiology and Biostatistics and Urology, University of California, San Francisco, San Francisco, CA 94158, USA
- ⁴⁸Department of Epidemiology and Biostatistics, School of Medicine, Case Western Reserve University, Wolstein Research Building, Cleveland, Ohio 44106, USA
- ⁴⁹Brigham and Women's Hospital, Dept. of Medicine, Sleep Medicine, 75 Francis Street, Boston, MA 02115, USA
- ⁵⁰Department of Medicine, Harvard Medical School, Boston, MA 02115, USA
- ⁵¹Jackson State University, 1400 Lynch Street, Jackson, MS 39217, USA
- ⁵²Tougaloo College, 500 West County Line Road, Tougaloo, MS 39174, USA
- ⁵³Departments of Epidemiology and Biostatistics, Harvard School of Public Health, Boston, MA 02115, USA
- ⁵⁴Dept. of Pediatrics, University of Pennsylvania School of Medicine, Philadelphia, Pennsylvania 19104, USA.
- ⁵⁵Department of Physiology and Biophysics, University of Mississippi Medical Center, 2500 N. State St., Jackson, MS 39216, USA

ACKNOWLEDGEMENTS

We are grateful to the participants who donated DNA samples, to David Altshuler, Jerome Buard, Kasia Bryc, Joseph Kovacs, Bernard de Massy, Gil McVean, Bogdan Pasaniuc and Sriram Sankararaman for conversations and critiques, and to Adam Auton for facilitating analysis of the 1000 Genomes Project data.

Analysis was supported by the Wellcome Trust and NIH grants HL084107 and GM091332.

CARe was supported by a contract from the National Heart, Lung and Blood Institute (HHSN268200960009C) to create a phenotype and genotype database for dissemination to the biomedical research community. Eight parent studies contributed phenotypic data and DNA samples through the Broad Institute (N01-HC-65226): the ARIC, CFS, CARDIA, JHS, and MESA studies, as well as the Cardiovascular Health Study (CHS), the Framingham Heart Study (FHS), and the Sleep Heart Health Study (SHHS). Support for CARe also came from the individual research institutions, investigators, field staff and study participants. Individual funding information is available at <http://public.nhlbi.nih.gov/GeneticsGenomics/home/care.aspx>.

All genome-wide genotyping of the CHOP dataset was supported by an Institutional Development Award to the Center for Applied Genomics from the Children's Hospital of Philadelphia, a research award from the Landenberger Foundation and the Cotswold Foundation. We thank all study participants and the staff at the Center for Applied Genomics for performing the genotyping.

AABCC was supported by a DoD Breast Cancer Research Program Era of Hope Scholar Award to CAH and the Norris Foundation, and by grants to the component studies: MEC (CA63464, CA54281); CARE (HD33175); WCHS (CA100598, DAMD 170100334, Breast Cancer Research Foundation); SFBC (CA77305, DAMD 17966071); CBCS (CA58223, ES10126), PLCO (NCI Intramural Research Program); NHBS (CA100374), WFBC (R01-CA73629) and CPS-II (the American Cancer Society).

AAPCC was supported by grants CA63464, CA54281, CA1326792, CA148085 and HG004726, and by grants to the component studies: PLCO (NCI Intramural Research Program), LAAPC (Cancer Research Fund 99-00524V-10258), both MEC and LAAPC (PC35139, DP000807); MDA (CA68578, CA140388, ES007784, DAMD W81XWH0710645); GECAP (ES011126); CaP Genes (CA88164); IPCG (W81XWH0710122); DCPC (GM08016, DAMD W81XWH0710203, DAMD W81XWH0610066); SCCS (CA092447, CA68485).

AALCC was supported by grants CA060691, CA87895, PC35145 and CA22453, CA68578, CA140388, ES007784, ES06717, CA55769, CA127219, CA1116460S1, CA1116460, CA121197, CA141716, CA121197S2, CPRIT RP100443, CA148127, DAMD W81XWH0710645, University Cancer Foundation, Duncan Family institute, Center for Community, Implementation, and Dissemination Research Core, and by grants to the component studies: PLCO and the Maryland Studies (NCI Intramural Research Program), LAAPC (Cancer Research Fund 99-00524V-10258), and both MEC and LAAPC (PC35139, DP000807).

REFERENCES

1. Jeffreys AJ, Kauppi L, Neumann R. Intensely punctate meiotic recombination in the class II region of the major histocompatibility complex. *Nat. Genet.* 2001; 29:217–212. [PubMed: 11586303]
2. McVean GA, et al. The fine-scale structure of recombination rate variation in the human genome. *Science.* 2004; 304:581–584. [PubMed: 15105499]
3. Myers S, Bottolo L, Freeman C, McVean G, Donnelly P. A fine-scale map of recombination rates and hotspots across the human genome. *Science.* 2005; 310:321–324. [PubMed: 16224025]
4. Kong A, et al. Fine-scale recombination rate differences between sexes, populations and individuals. *Nature.* 2010; 467:1099–1103. [PubMed: 20981099]
5. Kong A, et al. A high-resolution recombination map of the human genome. *Nature Genetics.* 2002; 31:241–247. [PubMed: 12053178]
6. Matise TC, et al. A second-generation combined linkage physical map of the human genome. *Genome Res.* 2007; 17:1783–1786. [PubMed: 17989245]
7. Weitkamp LR. Proceedings: Population differences in meiotic recombination frequency between loci on chromosome 1. *Cytogenet Cell Genet.* 1974; 13:179–182. [PubMed: 4208017]
8. Jorgenson E, et al. Ethnicity and human genetic linkage maps. *Am J Hum Genet.* 76; 2005:276–290.
9. Berg IL, et al. *PRDM9* variation strongly influences recombination hot-spot activity and meiotic instability in humans. *Nature Genetics.* 2010; 10:859–863. [PubMed: 20818382]

10. The 1000 Genomes Project Consortium. A map of human genome variation from population-scale sequencing. *Nature*. 2010; 467:1061–1073. [PubMed: 20981092]
11. Baudat F, et al. PRDM9 is a major determinant of meiotic recombination hotspots in humans and mice. *Science*. 2010; 327:836–840. [PubMed: 20044539]
12. Myers S, et al. Drive against hotspot motifs in primates implicates the *PRDM9* gene in meiotic recombination. *Science*. 2010; 327:876–879. [PubMed: 20044541]
13. Parvanov ED, Petkov PM, Paigen K. Prdm9 controls activation of mammalian recombination hotspots. *Science*. 2010; 327:835. [PubMed: 20044538]
14. Smith MW, et al. A high-density admixture map for disease gene discovery in African Americans. *Am J Hum Genet*. 2004; 74:1001–1013. [PubMed: 15088270]
15. Price AL, et al. Sensitive detection of chromosomal segments of distinct ancestry in admixed populations. *PLoS Genet*. 2009; 5:e1000519. [PubMed: 19543370]
16. Sankararaman S, Sridhar S, Kimmel G, Halperin E. Estimating local ancestry in admixed populations. *Am J Hum Genet*. 2008; 82:290–303. [PubMed: 18252211]
17. Patterson N, et al. Methods for high-density admixture mapping of disease genes. *Am J Hum Genet*. 2004; 74:979–1000. [PubMed: 15088269]
18. The International Haplotype Map Consortium. A second generation human haplotype map of over 3.1 million SNPs. *Nature*. 2007; 449:851–861. [PubMed: 17943122]
19. Freedman ML, et al. Admixture mapping identifies 8q24 as a prostate cancer risk locus in African-American men. *Proc Natl Acad Sci USA*. 2006; 103:14068–14073. [PubMed: 16945910]
20. Coop G, Wen X, Ober C, Pritchard JK, Przeworski M. High-resolution mapping of crossovers reveals extensive variation in fine-scale recombination patterns among humans. *Science*. 2008; 319:1395–1398. [PubMed: 18239090]
21. 1000 Genomes Project Consortium. A map of human genome variation from population-scale sequencing. *Nature*. 2010; 467:1061–1073. [PubMed: 20981092]
22. Myers S, Freeman C, Auton A, Donnelly P, McVean G. A common sequence motif associated with recombination hot spots and genome instability in humans. *Nat Genet*. 2008; 40:1124–1128. [PubMed: 19165926]
23. Kong A, et al. Sequence variants in the *RNF212* gene associate with genome-wide recombination rate. *Science*. 2008; 319:1398–1401. [PubMed: 18239089]
24. Reich DE, et al. Linkage disequilibrium in the human genome. *Nature*. 2001; 411:199–204. [PubMed: 11346797]
25. Raedt TD, et al. Conservation of hotspots for recombination in low-copy repeats associated with the *NFI* microdeletion. *Nat Genet*. 2006; 38:1419–1423. [PubMed: 17115058]
26. Li Y, Willer CJ, Ding J, Scheet P, Abecasis GR. MaCH: using sequence and genotype data to estimate haplotypes and unobserved genotypes. *Genetic Epidemiology*. 2010; 34:816–834. [PubMed: 21058334]

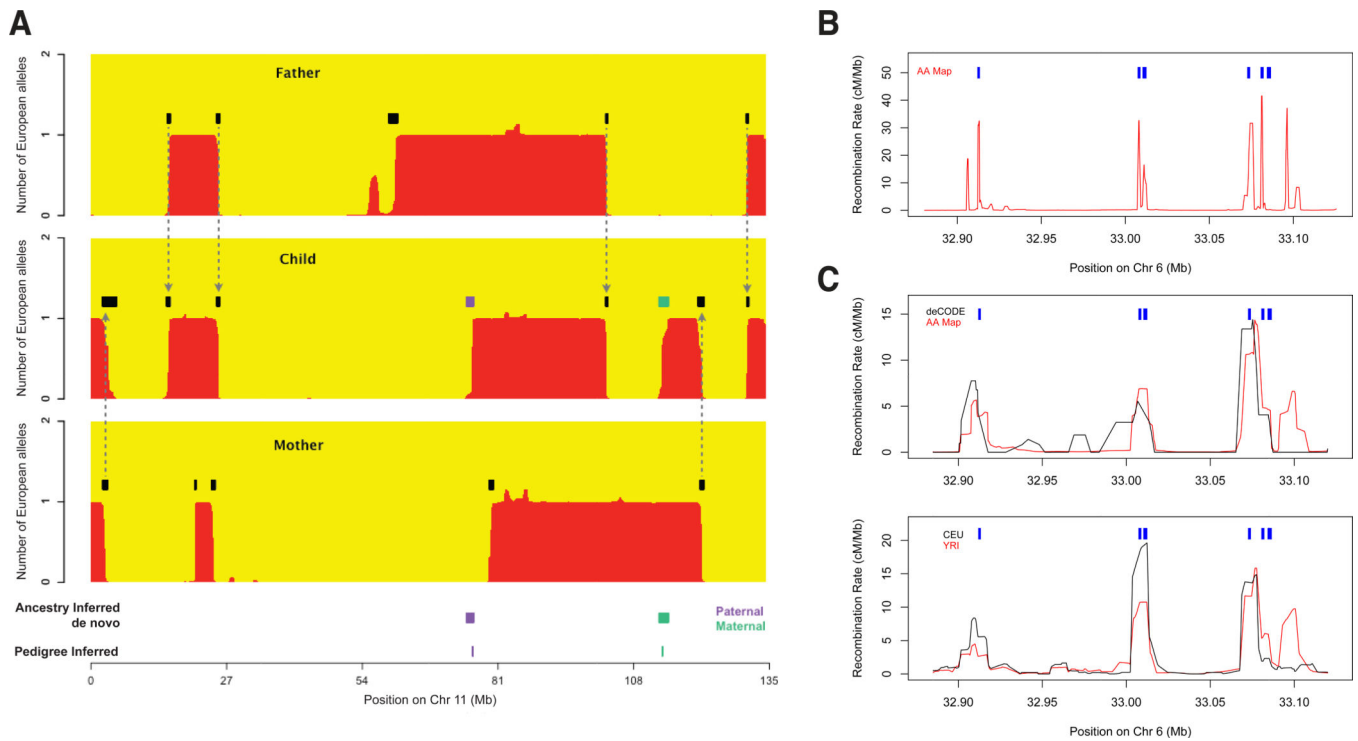


Figure 1.

Building an African American genetic map. (A) HAPMIX detection of crossovers between segments of inferred ancestry is illustrated in a father-mother-child trio. Black segments show inferred crossovers; arrows show transmission of ancestral crossovers from parent to child, Purple/green segments show *de novo* events (paternal/maternal origin respectively), corresponding to events identified directly using two additional children (bottom, “Pedigree inferred”). (B) The AA Map localizes five hotspots in a region of the MHC whose positions (blue) were previously mapped by sperm typing¹. (C) Comparison of maps shows a hotspot at 33.1Mb in the African-derived AA and YRI maps, but not the deCODE and CEU maps (all maps smoothed to 10kb).

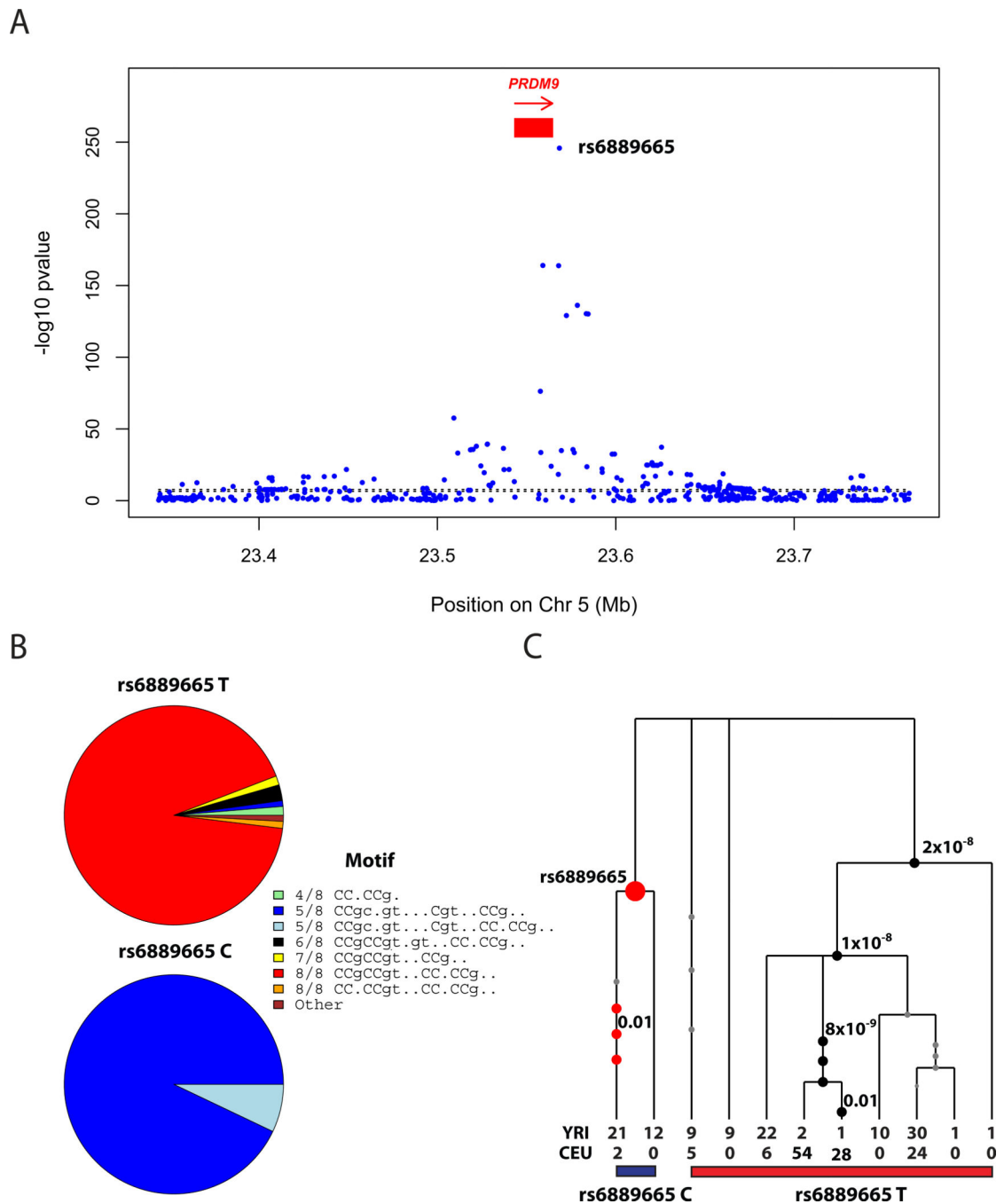


Figure 2. Association of *PRDM9* genetic variation with hotspot activity. (A) A GWAS measuring association of the “African-enrichment” (AE) phenotype shows a single genome-wide significant peak at *PRDM9*, with rs6889665 the best associated SNP. (B) Relationship between alleles at the rs6889665 and predicted binding target of the *PRDM9* zinc finger array⁹ for West African and European samples. The alleles are grouped into 8 clusters according to their best-matching region to the 13-bp motif, and annotated by the number of bases matching the motif. The African-enriched rs6889665 “C” allele always co-occurs with

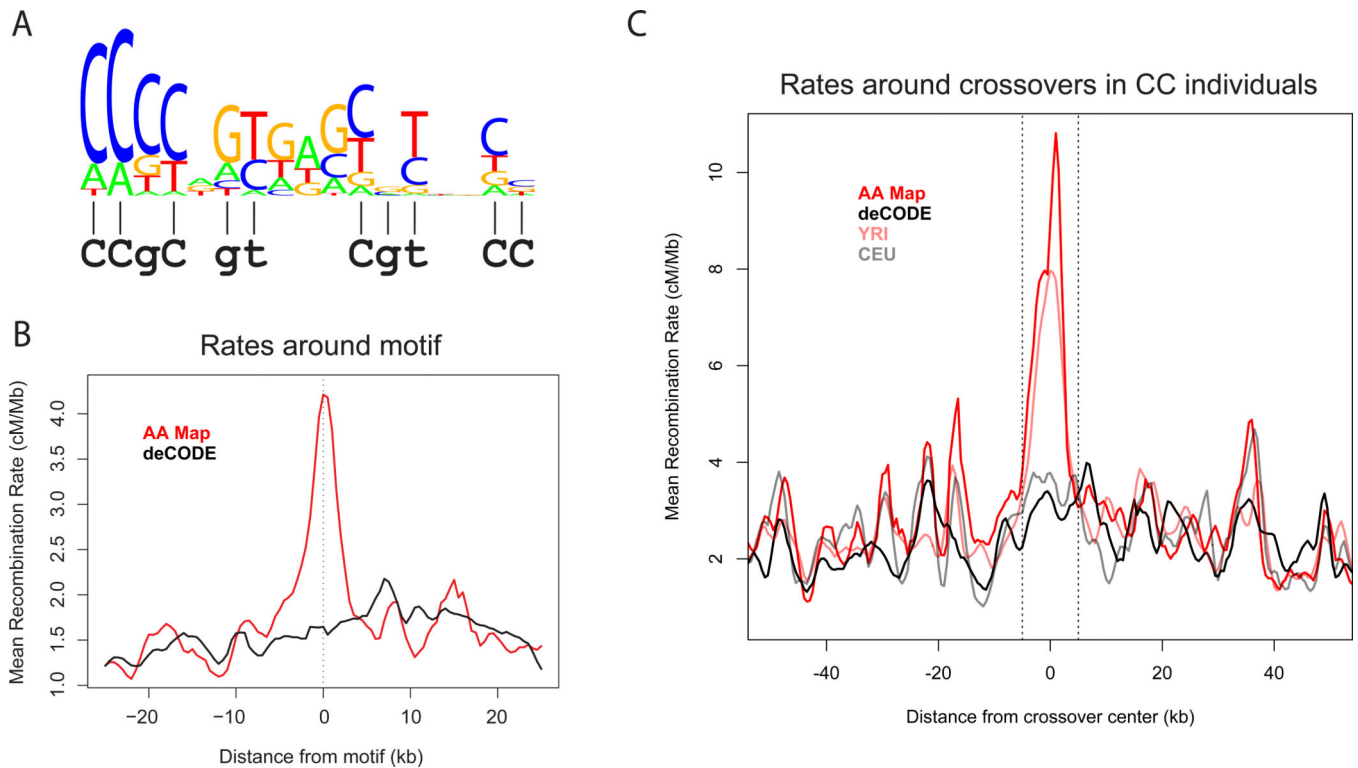
motifs with a poor (5/8) match to the 13-mer. (C) Gene tree³² of the LD block containing the *PRDM9* ZF array (Methods); numbered circles show SNPs and significant P-values for association, after conditioning on rs6889665.

Author Manuscript

Author Manuscript

Author Manuscript

Author Manuscript

**Figure 3.**

A sequence motif specifying the positions of African-enriched hotspots. (A) Logo plot showing a degenerate 17-bp hotspot motif, with stack height proportional to $-\log P$ -value, and relative letter height proportional to the mean crossover rate increase given each base. Below is the bioinformatic *PRDM9* binding prediction for the rs6889665 AE associated alleles (from Figure 2B), matching the motif at 10/11 bases (lines). (B) Average crossover rate (in 2 kb sliding windows) in the AA (red line) and deCODE (black line) maps surrounding the 500 strongest motif matches. (C) In seven rs6889665 “CC” individuals from the pedigree study, we localized 82 crossovers to within 10 kb, and plot average AA, YRI, deCODE and CEU map rates. There is no strong peak above local background in the deCODE or CEU maps.

Table 1

Genetic map assessments at different size scales

Scale (interval size)	ρ - Pearson correlation of the AA map (deCODE Map) to the specified LD map			Est. correlation of AA Map to the true map (inferred by MCMC)*	Est. coefficient of variation of AA Map (std. err. divided by crossover rate expected for interval size)*
	Combined LD [§]	CEU	YRI		
3 kb	0.75 (0.63)	0.66 (0.58)	0.71 (0.53)	0.93	1.41
10 kb	0.82 (0.74)	0.73 (0.70)	0.78 (0.65)	0.96	0.73
30 kb	0.86 (0.83)	0.78 (0.78)	0.83 (0.74)	0.98	0.36
100 kb	0.91 (0.89)	0.84 (0.85)	0.87 (0.81)	0.99	0.17
300 kb	0.94 (0.93)	0.89 (0.90)	0.92 (0.88)	1.00	0.08
1 Mb	0.97 (0.96)	0.94 (0.94)	0.95 (0.95)	1.00	0.04
3 Mb	0.98 (0.98)	0.97 (0.97)	0.98 (0.97)	1.00	0.02

Note: The numbers in this table are restricted to the autosomes and genomic segments more than 5 Mb from the telomere.

[§]The Combined map is the HapMap2 population-averaged LD-based map^{18,18}.

* The standard error of the map at each size scale is determined by the posterior probability distribution of the MCMC.